A Plug-in Type Integrated Rectenna Cell for Scalable RF Battery Using Wireless Energy Harvesting System

Manoj Kumar, *Graduate Student Member, IEEE*, Sundeep Kumar, *Graduate Student Member, IEEE*, Sagar Jain, and Ashwani Sharma, *Member, IEEE*

***Abstract*— Microwave power transfer is employed for charging self-sustainable internet of things (IoT) devices by wireless energy harvesting (WEH) using rectenna (Rx) and dedicated RF shower (Tx). The challenges for this implementation are the diverse power requirements of different devices and polarization and orientation mismatch between Tx and Rx. Different demands need redesigning rectennas, which can be avoided by scalable designs. A novel integrated rectenna devised as a plug-in-type unit cell is proposed for scalable RF battery. The plug-in feature allows multishape assemblies for the WEH system using multiple rectenna cells. This enables multiobjective-like dynamic power harvesting and orientation-insensitive operation. The rectenna cell designed with integrated matching has a high-gain endfire radiation pattern, which avoids blocking of incident waves and mutual coupling between adjacent rectennas. To illustrate scalability, linear-stacking and cuboid-shaped assemblies are evaluated for WEH performance. The results prove that the proposed scaling scheme with rectenna cells easily adapts to the user requirements.**

***Index Terms*— Internet of things (IoT), microwave power transfer, polarization, rectenna, scalability, wireless energy harvesting (WEH).**

I. Introduction

THE RF wireless energy harvesting (WEH) technique has gained a lot of attention in recent years for periodic recharging of sensor node batteries to achieve sustainability [1], [2]. The WEH-enabled nodes (Rx) convert the RF power into dc power using a rectenna module [3], which is sensitive to Rx orientation and RF power density. Moreover, various nodes may have diverse power requirements and size constraints for different application scenarios. This necessitates an innovative design with polarization-insensitive [4], [5], [6] and dynamic power harvesting [7] capabilities along with miniaturization [8], [9]. To target these requirements, a few scalable and orientation-insensitive WEH systems are proposed with multiport [10], multibeam [11], differential fed [12], and meta-material antennas [13].

For instance, a narrow beam 2-D quasi Yagi rectenna [11] with scalable directors and a miniaturized DRLA structure [14] for circular polarization are proposed. Furthermore, scalable differential WEH systems are designed in [15], [16], [17], [18], and [19] to enhance power harvesting capability by applying received RF waves in antiphase to the rectifying diode. Similarly, a flexible differential [20] and an integrated full-wave system [21] is proposed to design the scalable WEH system with improved harvesting capacity. The major limitations of these designs are their large prearranged footprints and complicated impedance matching with the rectifier circuit, rendering them unsuitable for internet of things (IoT) applications. Designs with integrated impedance matching also exist employing frequency selective surface (FSS) for scalablity and polarization-insensitive operation. For instance, FSS-based full-wave integrated dipole rectenna [22], tightly coupled antenna (TCA) [23], and stacked half-wave dipole FSS rectenna [24] are proposed with prearranged scalability to enhance power conversion efficiency (PCE). However, their large footprints and scalable but permanent structures make them unfavorable for adaptive WEH in a smart IoT scenario. For instance, in the application scenario exemplified in Fig. 1, the RF showers can be mounted on wall and ceiling with linearly or circularly polarized Tx antennas. Here, some sensors and IoT nodes demand different battery capacities with size constraints, and some nodes have varying orientations, whereas the others are exposed to horizontal as well as vertical impinging RF waves. Hence, the diverse RF battery requirements exist. Foremost, the available designs lack that kind of scalability feature, which allows the WEH systems to easily adapt to these requirements. The immediately mentioned requirements motivated the proposed work, and a plug-in-type rectenna module is designed with the following significant contributions.

1) The proposed rectenna acts as a unit cell for a scalable RF battery capable of adopting different geometrical formations according to the application scenario requirements.
2) A novel integrated endfire rectenna is designed with a compact footprint and high gain with better rectification capabilities.

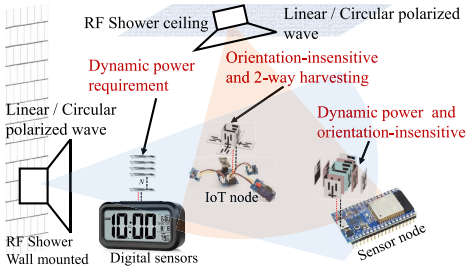

Fig. 1. Schematic of the scalable plug-in WEH system.

Manuscript received 28 July 2022; accepted 22 August 2022. This work was supported by the Science and Engineering Research Board, Department of Science and Technology, Government of India, under Grant ECR/2018/000343. *(Corresponding author: Ashwani Sharma.)*

The authors are with the Electrical Engineering Department, Indian Institute of Technology Ropar, Punjab 140001, India (e-mail: manojgarg@ieee.org; sundeep.19eez0004@iitrpr.ac.in; jainsagar927@gmail.com; ashwani.sharma@iitrpr.ac.in).

Color versions of one or more figures in this letter are available at https://doi.org/10.1109/LMWC.2022.3202711.

Digital Object Identifier 10.1109/LMWC.2022.3202711

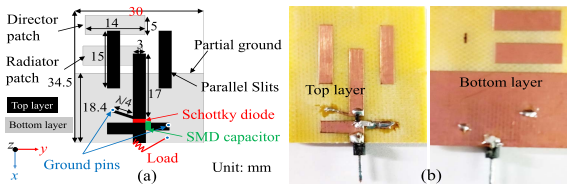

Fig. 2. (a) Layout of the proposed plug-in rectenna cell. (b) Fabricated prototype.

3) The plug-in rectenna module meets the orientation-insensitive and dynamic power harvesting requirements by incorporating different geometrical shapes.

II. Proposed Scalable WEH System

A. Plug-In-Type Integrated Rectenna Cell Design

The proposed rectenna cell is designed for the 5.8-GHz WEH system using the commercial ANSYS HFSS-2020-R1 on a double-sided low-cost FR4 substrate ($\epsilon_r = 4.4$ and $\tan\delta = 0.002$) having 1.565-mm thickness and 35-μm copper deposition. The rectenna layout is illustrated in Fig. 2, where the design comprises a novel high gain endfire antenna, a quarter-wave stub, a Schottky diode (SMS-7630-079LF), and an surface mount devices (SMD) capacitor. The conventional rectenna designs employ a matching network (MN) [25] and a dc low-pass filter (LPF) to achieve maximum power transfer from a 50-Ω matched antenna to the rectifier. However, distributed MN and LPF circuits contribute more to insertion loss as well as unfavorable for rectenna miniaturization. Therefore, the integrated rectenna having direct conjugate matching with rectifying diode instead of matching using loops and stubs minimizes insertion loss and complements miniaturization. To design an integrated rectenna, first, the impedance of the Schottky diode is evaluated at 5.8 GHz using the large-signal S-parameters (LSSP) technique for an input power of -10 dBm and 850-Ω load and noted as $Z_d = 26.93 - j92.84\ \Omega$. Furthermore, a novel high gain endfire antenna is designed to achieve conjugate matching with Z_d. A quarter-wave shorted stub is imposed at antenna port and diode junction for transforming the ground conductor to one dc terminal besides rejecting higher order harmonics to improve the PCE. A 100-pF shunt SMD capacitor is placed at the output terminal for dc power storage and filtering.

The proposed design is inspired from [26], [27], [28], and [29], which are endfire microstrip antennas. However, their intricate feeding systems make these designs unsuitable for rectenna application. In contrast, the proposed endfire antenna is designed with a proximity feed line enabling easy integration as a rectenna element, as illustrated in Fig. 2(a). The antenna bottom layer has a radiator and the director patch elements with a partial ground to direct the beam in the endfire direction. The upper layer has two parallel slits to achieve the desired directional radiation characteristics and matching. The proposed rectenna cell is fabricated using the MITS PCB prototyping machine, and the prototype is shown in Fig. 2(b). The antenna has a high gain (5.4 dBi), a wide half-power beamwidth of 113° in the xz plane, and a 66° beamwidth in the xy plane of RF patterns depicted in Fig. 3(a). The rectenna cell is simulated (measured) for dc power patterns to show a wide dc half-power beamwidth of 84° (86°) in the xz plane and 42° (40°) in the xy plane is plotted in Fig. 3(b) and (c), respectively. The simulated and measured patterns are in good agreement.

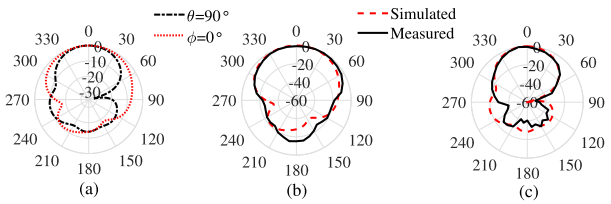

Fig. 3. (a) xy ($\theta = 90°$) and xz ($\phi = 0°$) RF patterns of the proposed antenna. Normalized harvested dc power pattern in (b) xy and (c) xz planes.

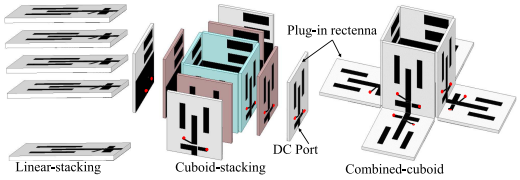

Fig. 4. Assembly of the plug-in rectenna modules for the scalable WEH system.

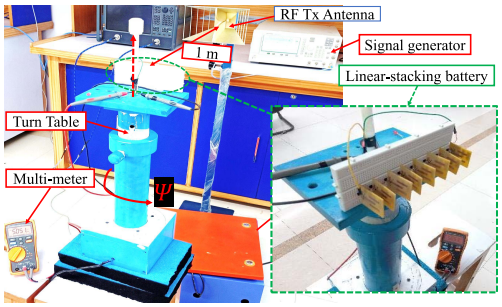

Fig. 5. Setup for dc pattern measurements and linear-stacking under test.

B. Scalable Assembly of the Proposed Rectenna Cells

A number of rectenna cells can be plugged-in to form various geometrical arrangements for RF battery based on the requirements. Here, three different assemblies are presented in Fig. 4, which achieves the following: 1) dynamic power harvesting using a linear-stacking battery; 2) orientation-insensitive dynamic power harvesting using a cuboid-stacking battery; and 3) two-way energy harvesting from horizontal as well as vertical waves along with orientation-insensitive operation using a combined-cuboid battery. A series dc combining technique is adopted to assemble the outputs of the cells. The performance is experimentally verified next.

III. Experiments and Results

The proposed rectenna cell and the composed sacalable assemblies are measured for WEH performance using the setup shown in Fig. 5, which includes an Agilent RF signal generator E8257D set to transmit 25-dBm signal at 5.8 GHz through a Tx horn antenna (linearly polarized) with 8.6-dBi gain imitating a wall mounted RF shower. Furthermore, the RF wave power density impinging on the proposed rectenna aperture is 0.217 W/m^2. The WEH system is mounted 1 m away from the Tx on an automated turn table for dc pattern measurements using a Keysight U1232A multimeter. First, the dc voltage across the varying load is measured, as shown in Fig. 6(a), showing a rectenna efficiency of 71% at the optimal load of 700 Ω for a single rectenna cell. The corresponding measured dc power patterns of a single rectenna cell are discussed earlier in Fig. 3(b) and (c).

A. Linear-Stacking Measurements

Multiple plug-in rectenna cells are assembled and connected through a breadboard for measuring the performance of the linear-stacking battery whose prototype is shown in Fig. 5 (inset). The stacked assembly of up to eight cells is measured

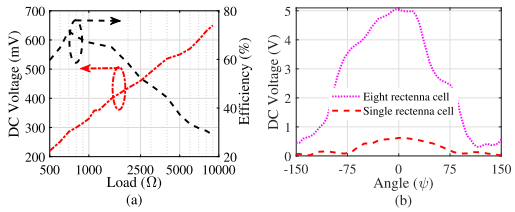

Fig. 6. Measured (a) dc voltage and efficiency versus load for single rectenna and (b) dc pattern of linear-stacking assembly.

TABLE I

LINEAR STACKING FOR DYNAMIC HARVESTING WITH INCREASING CELLS

Stacked rectennas	1	2	3	4	5	6	7	8
DC Voltage (mV)	660	1300	1826	2489	3240	3901	4489	5051

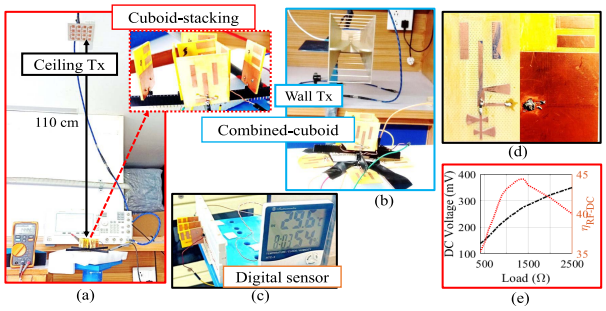

Fig. 7. Measurement setup for (a) cuboid stacking and (b) combined cuboid. (c) Real demonstration by powering a digital sensor. (d) Fabricated prototype with MN. (e) RF-dc efficiency with MN.

for the dc open-circuit voltage. The results are listed in Table I for increasing the number of rectenna cells to demonstrate the dynamic harvesting capability. The results indicate that a single cell has 660-mV output, which gradually increases to 5051 mV for eight-cells stacking. A little low additive scaling in harvested dc for increasing number of cells can be attributed to connection losses. The angular harvesting performance of the linear-stacking battery is measured by rotating the turn table in azimuth ψ with 5° steps, and the measured dc patterns are plotted in Fig. 6(b) for single-cell and eight-cells assembly showing that the proposed approach can meet the scaled power requirements of various nodes.

B. Cuboid-Stacking and Combined-Cuboid Measurements

Since the cuboid stacking and combined cuboid harvest from vertical waves, the measurement setup facilitating this is shown in Fig. 7(a) and (b), which uses a planer array (linearly polarized) with 8.6-dBi gain as Tx imitating a ceiling mounted RF shower besides the original horn Tx on wall. The cuboid stacking can harvest from only ceiling RF shower, whereas combined cuboid harvests from the both. The angular harvesting performance is measured, and polarization mismatching due to orientation of the node is expected. However, the results depicted in Fig. 8(a) displaying the measured dc patterns indicate that these assemblies have good tolerance for orientation misalignment and polarization mismatch. Moreover, the combined cuboid is able to harvest energy from vertical as well as horizontal source with good angular coverage. A real application is also demonstrated in Fig. 7(c) by powering a digital sensor with temperature and pressure monitoring in real scenario. The digital sensor is powered directly from the proposed linear stacking where three cells of the proposed rectenna are sufficient for battery-less operation.

The mutual coupling effects are also under limits, as presented in Fig. 8(b), where the isolation between the adjacent antenna elements is 26 dB in the linear stacking for a 10-mm

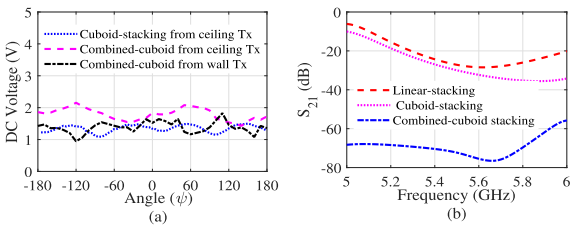

Fig. 8. (a) Cuboid-stacking and combined-cuboid batteries assembled from the proposed rectenna cell. (b) Mutual coupling.

TABLE II

COMPARISON WITH STATE OF THE ART

Ref.	Technique	Frequency (GHz)	Scalablity	η_{rf-dc} (%)
[19]	Differential	2.45 5.8	Permanent design	36.4 @2.48 GHz 6.2 @5.96 GHz
[20]	Differential	5.8	Permanent	27 @5.8 GHz
[21]	Meta-material	2.45	Permanent	74 @2.45 GHz
[30]	Monopole	0.866	Scalable fixed operation	28.4 @0.866 GHz
Proposed design	Unit-cell Integrated	5.8	Scalable dynamic operation	71 @5.8 GHz

interelement distance; the same is 35 and 65 dB in the cuboid stacking and the combined cuboid, respectively. To showcase efficiency improvement by utilizing integrated rectenna design, the proposed antenna with 50-Ω input impedance is also designed. The 50-Ω antenna has an RF gain of 5 dBi, which is equivalent to the corresponding integrated design. Fig. 7(d) shows the fabricated prototype with the MN and filter circuit [25]. The rectenna with MN harvests 267 mV with an optimal load of 1300 Ω and achieves the RF-dc efficiency of 44.20%, as shown in Fig. 7(e). This validates the benefit of utilizing the integrated topology of the rectenna design. A comparison with the most pertinent works [19], [20], [21], [30] is performed in Table II. The differential rectenna element designed in [19] and the integrated sheet with full-wave rectifier circuit proposed in [21] have large prearranged footprints with permanent-type scalability. Whereas, the 1×3 horizontal and vertical stacked WEH system proposed in [30] has limited geometrical arrangements due to omnidirectional RF pattern. This is because in [30], a large interelement distance is required to avoid mutual coupling resulting in a large dimension; moreover, RF blocking is a major issue due to omnidirectional radiation pattern. Therefore, achieving scalability along with tolerance for polarization and orientation mismatching is not possible conveniently within constrained size requirement of IoT nodes.

IV. CONCLUSION

A novel integrated miniaturized plug-in rectenna cell having endfire pattern is presented for orientation-insensitive dynamic power harvesting capability at IoT sensor nodes. The proposed rectenna cell has a high RF gain of 5.4 dBi with wide RF 3-dB beamwidth of 113° and 66° in two orthogonal planes, respectively. This results in the corresponding dc beamwidth of 86° and 40°. The scalable linear-stacking battery formed by eight rectenna cells harvests 5051 mV against 660 mV harvested by a single cell, which exhibits dynamic harvesting capability. Similarly, the cuboid and combined-cuboid stackings show good tolerance against orientation and polarization mismatching along with dynamic power harvesting. The low mutual coupling of ≤ -26 dB between adjacent rectennas enabled compact stacking structures for size constrained IoT sensor nodes. Hence, the proposed plug-in strategy enhances harvested dc power and mitigates polarization and orientation mismatch issues in WEH systems.

REFERENCES

[1] Z. Liang and J. Yuan, "A compact dual-band four-port ambient RF energy harvester with high-sensitivity, high-efficiency, and wide power range," *IEEE Trans. Microw. Theory Techn.*, vol. 70, no. 1, pp. 641–649, Jan. 2022.

[2] C. Liu, H. Lin, Z. He, and Z. Chen, "Compact patch rectennas without impedance matching network for wireless power transmission," *IEEE Trans. Microw. Theory Techn.*, vol. 70, no. 5, pp. 2882–2890, May 2022.

[3] S. F. Bo, J.-H. Ou, Y. Dong, S.-W. Dong, and X. Y. Zhang, "All-polarized wideband rectenna with enhanced efficiency within wide input power and load ranges," *IEEE Trans. Ind. Electron.*, vol. 69, no. 7, pp. 7470–7480, Jul. 2022.

[4] S. F. Bo, J.-H. Ou, J. W. Wang, J. Tang, and X. Y. Zhang, "Polarization-independent rectifier with wide frequency and input power ranges based on novel six-port network," *IEEE Trans. Microw. Theory Techn.*, vol. 69, no. 11, pp. 4822–4830, Nov. 2021.

[5] L. Li, X. Zhang, C. Song, W. Zhang, T. Jia, and Y. Huang, "Compact dual-band, wide-angle, polarization-angle-independent rectifying metasurface for ambient energy harvesting and wireless power transfer," *IEEE Trans. Microw. Theory Techn.*, vol. 69, no. 3, pp. 1518–1528, Mar. 2021.

[6] Y. Wei *et al.*, "A multiband, polarization-controlled metasurface absorber for electromagnetic energy harvesting and wireless power transfer," *IEEE Trans. Microw. Theory Techn.*, vol. 70, no. 5, pp. 2861–2871, May 2022.

[7] A. Dolgov, R. Zane, and Z. Popović, "Power management system for online low power RF energy harvesting optimization," *IEEE Trans. Circuits Syst. I, Reg. Papers*, vol. 57, no. 7, pp. 1802–1811, Jul. 2010.

[8] M.-J. Nie, X.-X. Yang, G.-N. Tan, and B. Han, "A compact 2.45-GHz broadband rectenna using grounded coplanar waveguide," *IEEE Antennas Wireless Propag. Lett.*, vol. 14, pp. 986–989, 2015.

[9] C. Song *et al.*, "Matching network elimination in broadband rectennas for high-efficiency wireless power transfer and energy harvesting," *IEEE Trans. Ind. Electron.*, vol. 64, no. 5, pp. 3950–3961, May 2017.

[10] Z. Popović *et al.*, "Scalable RF energy harvesting," *IEEE Trans. Microw. Theory Techn.*, vol. 62, no. 4, pp. 1046–1056, Apr. 2014.

[11] Y.-S. Chen and J.-W. You, "A scalable and multidirectional rectenna system for RF energy harvesting," *IEEE Trans. Compon., Packag., Manuf. Technol.*, vol. 8, no. 12, pp. 2060–2072, Dec. 2018.

[12] T. Sakamoto, Y. Ushijima, E. Nishiyama, M. Aikawa, and I. Toyoda, "5.8-GHz series/parallel connected rectenna array using expandable differential rectenna units," *IEEE Trans. Antennas Propag.*, vol. 61, no. 9, pp. 4872–4875, Sep. 2013.

[13] F. Erkmen and O. M. Ramahi, "A scalable, dual-polarized absorber surface for electromagnetic energy harvesting and wireless power transfer," *IEEE Trans. Microw. Theory Techn.*, vol. 69, no. 9, pp. 4021–4028, Sep. 2021.

[14] B. Strassner, S. Kokel, and K. Chang, "5.8 GHz circularly polarized low incident power density rectenna design and array implementation," in *IEEE Antennas Propag. Soc. Int. Symp., Dig., USNC/CNC/URSI North Amer. Radio Sci. Meeting*, Jun. 2003, pp. 950–953.

[15] T. Matsunaga, E. Nishiyama, and I. Toyoda, "5.8-GHz stacked differential mode rectenna suitable for large-scale rectenna arrays," in *Proc. Asia–Pacific Microw. Conf. Proc. (APMC)*, Nov. 2013, pp. 1200–1202.

[16] T. Matsunaga, E. Nishiyama, and I. Toyoda, "5.8-GHz stacked differential rectenna suitable for large-scale rectenna arrays with DC connection," *IEEE Trans. Antennas Propag.*, vol. 63, no. 12, pp. 5944–5949, Dec. 2015.

[17] A. Mavaddat, S. H. M. Armaki, and A. R. Erfanian, "Millimeter-wave energy harvesting using 4×4 microstrip patch antenna array," *IEEE Antennas Wireless Propag. Lett.*, vol. 14, pp. 515–518, 2015.

[18] K. Yasuda, E. Nishiyama, and I. Toyoda, "A high efficiency differential rectenna employing two-parasitic-element stacked antenna," in *Proc. Asia–Pacific Microw. Conf. (APMC)*, Nov. 2018, pp. 132–134.

[19] K. Saito, E. Nishiyama, and I. Toyoda, "A 2.45- and 5.8-GHz dual-band stacked differential rectenna with high conversion efficiency in low power density environment," *IEEE Open J. Antennas Propag.*, vol. 3, pp. 627–636, 2022.

[20] Y. Ushijima, T. Sakamoto, E. Nishiyama, M. Aikawa, and I. Toyoda, "5.8-GHz integrated differential rectenna unit using both-sided MIC technology with design flexibility," *IEEE Trans. Antennas Propag.*, vol. 61, no. 6, pp. 3357–3360, Jun. 2013.

[21] F. Erkmen, T. S. Almoneef, and O. M. Ramahi, "Electromagnetic energy harvesting using full-wave rectification," *IEEE Trans. Microw. Theory Techn.*, vol. 65, no. 5, pp. 1843–1851, May 2017.

[22] F. Erkmen, T. S. Almoneef, and O. M. Ramahi, "Scalable electromagnetic energy harvesting using frequency-selective surfaces," *IEEE Trans. Microw. Theory Techn.*, vol. 66, no. 5, pp. 2433–2441, May 2018.

[23] T. S. Almoneef, F. Erkmen, M. A. Alotaibi, and O. M. Ramahi, "A new approach to microwave rectennas using tightly coupled antennas," *IEEE Trans. Antennas Propag.*, vol. 66, no. 4, pp. 1714–1724, Apr. 2018.

[24] T. S. Almoneef, H. Sun, and O. M. Ramahi, "A 3-D folded dipole antenna array for far-field electromagnetic energy transfer," *IEEE Antennas Wireless Propag. Lett.*, vol. 15, pp. 1406–1409, 2016.

[25] M. Kumar, S. Kumar, and A. Sharma, "Dual-purpose planar radial-array of rectenna sensors for orientation estimation and RF-energy harvesting at IoT nodes," *IEEE Microw. Wireless Compon. Lett.*, vol. 32, no. 3, pp. 245–248, Mar. 2022.

[26] Y. Luo, Q.-X. Chu, and J. Bornemann, "A differential-fed Yagi–Uda antenna with enhanced bandwidth via addition of parasitic resonator," *Microw. Opt. Technol. Lett.*, vol. 59, no. 1, pp. 156–159, Jan. 2017.

[27] M. Farran *et al.*, "Compact quasi-Yagi antenna with folded dipole fed by tapered integrated balun," *Electron. Lett.*, vol. 52, no. 10, pp. 789–790, 2016.

[28] S. S. Jehangir and M. S. Sharawi, "A miniaturized UWB biplanar Yagi-like MIMO antenna system," *IEEE Antennas Wireless Propag. Lett.*, vol. 16, pp. 2320–2323, 2017.

[29] Y. Luo and Q.-X. Chu, "A Yagi–Uda antenna with a stepped-width reflector shorter than the driven element," *IEEE Antennas Wireless Propag. Lett.*, vol. 15, pp. 564–567, 2016.

[30] S. D. Assimonis, S.-N. Daskalakis, and A. Bletsas, "Sensitive and efficient RF harvesting supply for batteryless backscatter sensor networks," *IEEE Trans. Microw. Theory Techn.*, vol. 64, no. 4, pp. 1327–1338, Apr. 2016.